WAPD-T-3042

Conf-950835--1

VAPOR FRACTION MEASUREMENTS IN A STEAM-WATER DUCT AT ATMOSPHERIC PRESSURE USING NEUTRON RADIOGRAPHY

S. S. Glickstein, J. H. Murphy & R. B. Hammond

Westinghouse Electric Corporation
Bettis Atomic Power Laboratory
Post Office Box 79
West Mifflin, PA 15122

For Submission To

ASME Fluids Engineering Division Summer Meeting
Flow Visualization and Image Processing of Multiphase Systems
Hilton Head, SC

August 1995

DISCLAIMER

Portions of this document may be illegible in electronic image products. Images are produced from the best available original document.

VAPOR FRACTION MEASUREMENTS IN A STEAM-WATER DUCT AT ATMOSPHERIC PRESSURE USING NEUTRON RADIOGRAPHY

S. S. Glickstein, J. H. Murphy & R. B. Hammond

ABSTRACT

Real-time neutron radiography has been used to study the dynamic behavior of two-phase flow and measure vapor fractions in a steam-water duct at atmospheric pressure. This unique experimental technique offers one the opportunity to observe and record on videotape flow patterns and transient behavior of two-phase flow inside opaque containers without perturbing the environment. The neutron radiographic technique is non-intrusive and requires no special transparent window region. Data are recorded simultaneously over a large area of interest. Image processing of the video data can be employed to measure bubble velocities and time-averaged and instantaneous vapor fractions.

I. INTRODUCTION

Real-time neutron radiography is being employed as part of a fundamental fluids test program designed to isolate specific phenomena necessary for computer model development and to obtain data needed to develop the models. It is also intended to be used to augment the computer modeler's understanding of two-phase flow phenomena. Standard optical techniques cannot normally be used to observe the dynamic behavior of two phase flow within a metal test section. The metal test section is necessary to extend testing to high pressures. Gamma attenuation techniques have been used to measure vapor fractions at distinct points inside such an enclosure (1). However with the advent of real time-neutron radiography (now officially termed neutron radioscopy) the experimenter is offered a unique means of recording on videotape the instantaneous dynamic behavior of the gas-liquid mixture over a large area of the test region. Image processing techniques provide a means of extracting quantitative measurements from the video data.

Several investigators have used this methodology with air-water systems (2-6). Hibiki (6) has reported void fraction results in good agreement with probe measurements and with drift flux model correlations. He has also reported observing two-phase steam-water flow inside a heated round tube. The extraction of precise quantitative results from neutron radiographs is complicated by the fact that neutron removal from the water is mainly due to the scattering process; thus neutrons removed from one water region may show up in another part of the image. Glickstein et al have shown that Monte Carlo computer simulation of the radiographic experiment can be used to understand this phenomenon (7) and a method correcting for such scattering effects has been developed. To substantiate the reliability of the neutron radiographic technique to measure precise vapor fractions in steam-water conditions of varying pressures and temperatures (where the relative densities of the water and steam are on the order of 10:1 or less as compared to 1600:1 at atmospheric pressure) rotating acrylic disc with holes were used to simulate bubble flow (8). The results of these experiments demonstrated the importance of neutron scattering and substantiated that vapor fraction measurements can be determined reliably and with high precision.

This paper extends the authors' previous time-averaged vapor fraction measurements in an air-water loop (2) to steam-water conditions at atmospheric pressure. A brief description of the experimental arrangement is presented in the next section. To explore the range of operational

capability of the flow loop for atmospheric testing, the input heat to the test section, inlet flow rate and inlet temperature conditions were varied as shown in Table 1. The results of the experiments are discussed in Section III.

II. EXPERIMENT

The experiments were performed at the Pennsylvania State University Research Reactor Facility using a Precise Optics real-time neutron radiographic camera shown in Figure 1. It has a field of view of approximately 230 mm. A side view of the reactor and the experimental test apparatus is shown in Figure 2. A portable test loop was constructed that could be moved in and out of the beam port area with ease. The loop can be raised and lowered remotely which allows for measurements to be made over the entire length of the duct. The duct can also be inclined. The duct was 2.5 mm thick, 57 mm wide, 690 mm long and was made of 1.5 mm thick stainless steel that was heated electrically using an 80 kW arc welding power source unit capable of providing 1500A to the test section. A diesel generator installed outside the reactor building was required to power the welding unit. Because of the high currents needed to heat the test section magnetic fields on the order of 10 Gauss were present at the camera position. A special mu metal shield was constructed and placed around the camera to eliminate perturbations in the video signal due to the magnetic field.

At the maximum 1 MW steady state reactor operating conditions of the TRIGA reactor, the thermal neutron beam at the test section was on the order of 2×10^6 n/cm^2/s. The L/D ratio was approximately 55. Directing the beam through the thin duct dimension, the dynamic behavior of the steam-water flow is clearly visible through the stainless steel duct and alumina insulator backup support structure. The neutron radiography data were recorded on video tape as a series of discrete frames at a rate of 30 frames per second. Approximately 6 minutes of data are recorded for each run. The experimental conditions for each test are shown in Table 1. Each frame of the videotape shows a gray scale representation of a portion of the test section with the gray level at any point being an indication of the relative proportion of liquid versus vapor. Each of these segments is then time-averaged (8192 frames, corresponding to 4.55 minutes of data acquisition) and digitized. The result is a file containing a matrix of gray scale values. The matrix represents 480 pixels in the vertical direction and 512 pixels in the horizontal direction. (The test region was represented by 480x160 pixels.) The digitized data were normalized to compensate for differences in the intensity of the neutron source beam from one run to another as well as for the response characteristics of the camera. The normalization was done by selecting a distinct reference point on the digitized picture which should have the same gray scale value for every run, independent of test conditions. Every 10 rows in the matrix were averaged to produce a smaller matrix that was 48 rows by 160 columns. (Each horizontal row represented a 4.8 mm width of the test section and a vertical row 0.5 mm.) To compute vapor fractions, the gray scale value of the liquid-vapor mixture must be compared to the gray scale values for the same point with the test section completely filled with water (no boiling) and with the test section completely empty. The average void fraction (neglecting scattering effects) VF(x,y), can be determined from the gray scale measurements and is given by the following relation:

$$VF(x,y) = \frac{1 - \dfrac{\ln\{V(x,y)/[E(x,y)]\}}{\ln\{[W(x,y)]/[E(x,y)]\}}}{1 - (\mu_v/\mu_w)} \qquad (1)$$

where

$V(x,y)$ = the time-averaged gray scale of the duct at operating conditions,
$W(x,y)$ = the time-averaged gray scale of the duct filled with water, no boiling
$E(x,y)$ = the time averaged gray scale of the empty duct,
μ_v/μ_w = ratio of vapor-to-water attenuation coefficient.

When the effects of neutron scattering within the duct are included, equation (1) takes the following form:

$$VF(x,y) = \frac{1 + \dfrac{\ln [1 - P(x,y)]}{\sigma_t N_w T(x,y)}}{1 - (N_v/N_w)} \qquad (2)$$

where

$P(x,y)$ = the collision probability in a vapor-water mixture and is a function of $V(x'y')$, $W(x',y')$ and $E(x',y')$, where (x',y') are summed over the entire test region,
σ_t = the microscopic total hydrogen cross section,
N_v = the hydrogen number density in vapor,
N_w = the hydrogen number density in water, and
$T(x,y)$ = the thickness of the water duct.

The vapor fraction is then computed for each pixel point and stored in a disk file for subsequent use. PV-Wave (9) has been used for displaying the results graphically. The data acquisition and reduction process is shown in Figure 3.

III. RESULTS

A typical time-averaged radiograph of a 20 cm length of test section is shown Figure 4. The time-averaged vapor fraction results extracted from the gray level distribution from this region of the radiograph is displayed in Figure 5. The top and bottom 1.27 cm section of the image appeared to have some anomalies attributed to falloff in the response function of the camera along the outer edge. The region was therefore omitted. Figure 6 shows line graph results for several radial positions along the test section.

The results shown in Figure 7 confirm the expected trends in increased vapor fraction with increased heat input. Several other experimental results at other operating conditions are shown in Figure 8. The presence of pressure taps and thermocouples located on the front surface of the test section and holes in the structure to allow their passage perturbed the measured result at each tap and thermocouple location. The effect is noted as a slight increase or decrease in the value of the vapor fraction at that position.

During initial testing, unique pictures were captured of individual nucleation sites at low input heat conditions as shown in Figure 9. These pictures reveal the power of neutron radioscopy to capture events that would probably have been missed had pointwise measurements been performed using traditional techniques. These particular nucleation sites have been reproduced periodically implying a probable imperfection on the surface of the wall.

In addition to the vertical tests, some preliminary runs have been made with the duct inclined edge-up 15°. Typical results are shown in Figure 10.

The vapor fractions shown on Figures 5-8 have been compared to calculations. Those comparisons reveal that the vapor fractions becomes significant well before the bulk fluid has reached saturation enthalpy. Much of the vapor generation, therefore, is due to subcooled boiling.

IV. SUMMARY & CONCLUSIONS

Experimental studies to support the methodology for measuring vapor fractions using neutron radioscopy techniques have been presented. Results of a series of tests designed to measure vapor fraction in a heated test section taken under different operating conditions confirm expected trends in increased vapor fraction with increased heat input and reduced fluid flow rate. The ability to view a large region of the test section instantaneously and to view in real-time the dynamic behavior of the fluid enables one to record data, such as the location of nucleation sites not readily captured by any other technique.

ACKNOWLEDGEMENT

The authors would like to extend their sincere appreciation to the members of the Pennsylvania State University reactor staff for their support and cooperation during the course of this experiment. A special note of thanks to Robert Gould for his significant support with the operation of the neutron radiographic camera and for his many helpful suggestions during this investigation.

REFERENCES

1. O. C. Jones and J. M. Delhaye, "Transient and Statistical Measurement Techniques For Two-Phase Flows: A Critical Review," Int. J. Multiphase Flow, Vol. 3, pp 89-116, Dec. 1976

2. S. S. Glickstein, W. H. Vance and H. Joo, " Vapor Fraction Measurements Using Neutron Radiography," Transactions of the ANS/ENS, Vol. 66 Nov. 1992

3. S. Fujine et al, "Study of Visualization of Fluid Phenomena Using Neutron Radiography Technique," Proceedings of the Fourth World Conference on Neutron Radiography, May 1992

4. K. Mishima, T. Hibiki and H. Nishihara, "Some Characteristics of Gas-Liquid Flow in Narrow Rectangular Ducts," Int. J. Multiphase Flow, Vol. 19, pp 115-124, Feb. 1993

5. N. Takenaka et al, "Application of Real-Time Neutron Radiography To Multiphase Flow Visualization and Measurement," Proceedings of the Third World Conference on Neutron Radiography, May 1989

6. T. Hibiki et al, "Study of Two-Phase Flow Using Image Processing Technique," Proceedings of the Fourth World Conference on Neutron Radiography, May 1992

7. S. S. Glickstein, H. Joo and W. H. Vance, "Interpreting Neutron Radiographs Via Computer Simulation," Proceedings of the Fourth World Conference on Neutron Radiography, May 1992

8. S. S. Glickstein, H. Joo, W. H. Vance and J. H. Murphy, " Void Fraction Measurements of Acrylic Discs via Neutron Radiography," Transactions of the ANS, Vol. 70, June 1994

9. PV-WAVE, Visual Numerics Inc., Boulder CO

TABLE 1
NEUTRON RADIOGRAPHY DATA
AUGUST 10-13, 1993

Run Number	Nom Flow (gpm)	T_{in} (°F)	Power* (W)	Remarks
97	0.5	160	3480	No camera magnetic shield
98	0.5	160	3480	Camera shield in place
99	0.5	190	1170	No boiling; Background run
100	0.5	190	1370	Slight boiling
101	0.5	198	1700	Continuous boiling
102	0.0	198	80	Empty
103	0.5	160	2770	
104	0.5	160	2340	Background full, no boiling
105	0.5	160	2940	
106	0.5	160	3100	
107	0.5	160	3290	
108	0.5	160	3450	
109	0.5	160	3600	
110	0.5	160	3940	
111	0.5	160	4720	
112	0.5	160	80	Background full, no boiling
113	0.0	160	0	Drained during run
114	0.0	160	90	Filled during run
115	0.5	160	3230	Background full, no boiling
116	0.8	160	6870	Max power
117	0.8	160	5920	
118	0.8	160	6160	
119	0.8	160	6410	
120	0.8	160	6680	
121	0.8	195	3100	
122	0.8	195	3420	
123	0.8	195	3760	
124	0.8	195	4140	
125	0.8	180	1970	Background full, no boiling
126	0.0	180	100	Empty
127	0.0	120	95	Empty
128	0.25	120	95	Background full, no boiling
129	0.25	160	2090	
130	0.25	160	2350	
131	0.25	160	2630	
132	0.25	160	2930	

* Includes estimated 400W to 600W heat loss

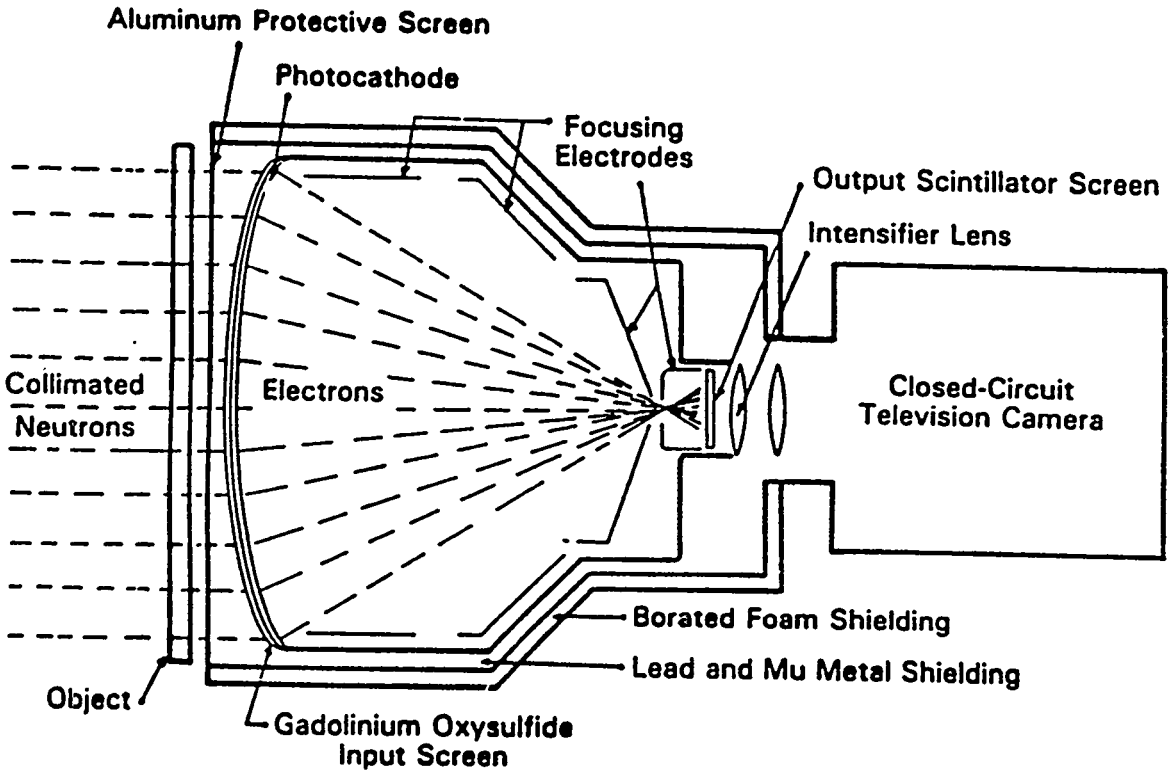

Figure 1 Precise Optics neutron radiography camera

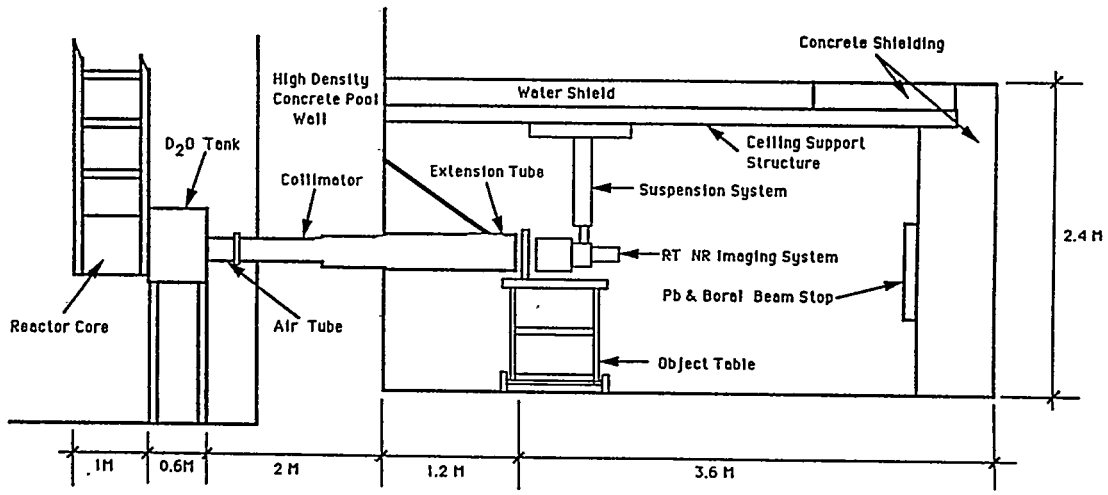

(a)

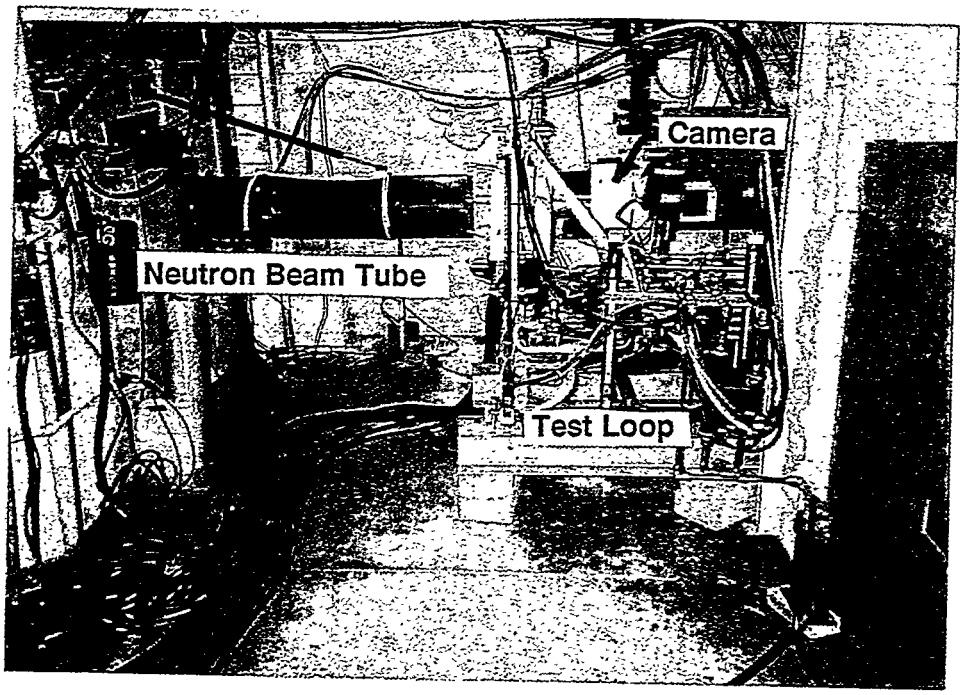

(b)

Figure 2 a) Side view of the Penn State Reactor beam hole laboratory
b) Flow loop in position during neutron radiography testing.

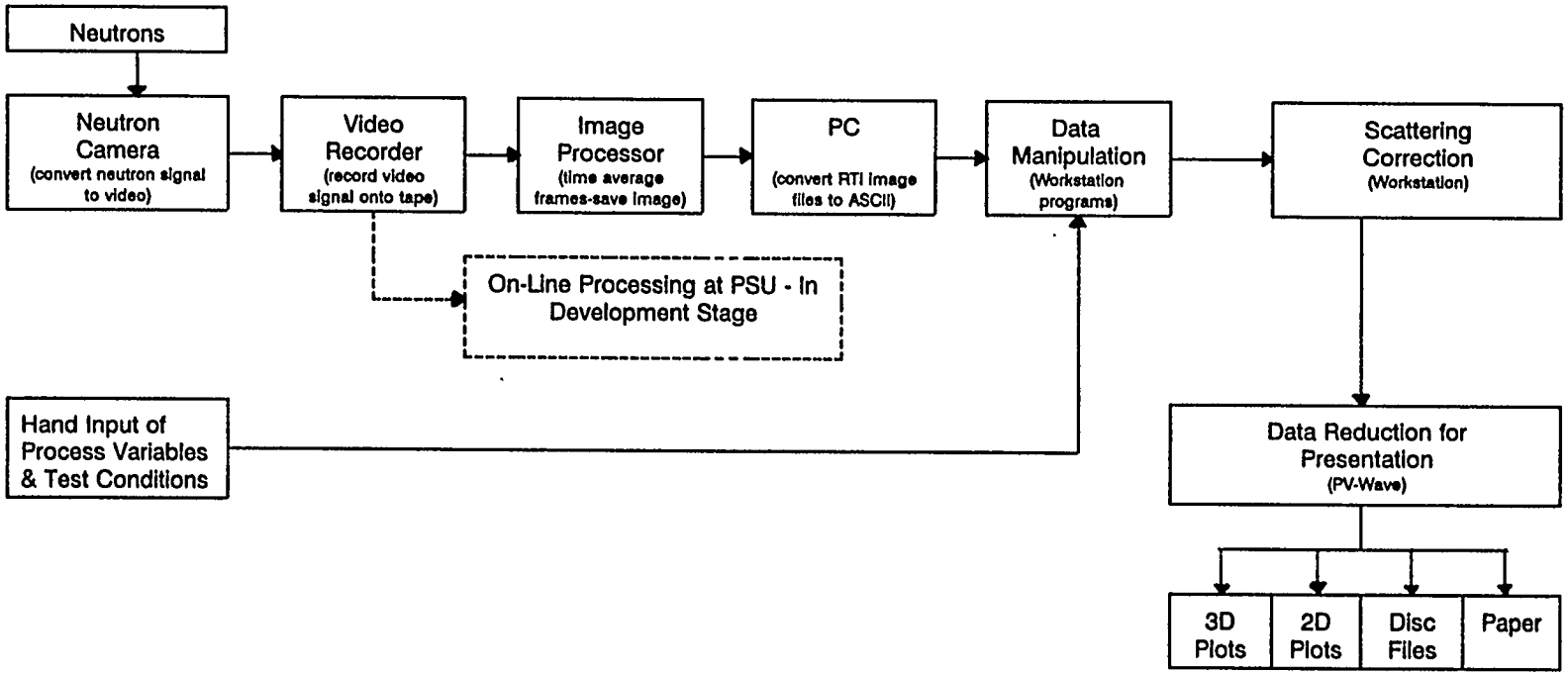

Figure 3 Data acquisition and data reduction process.

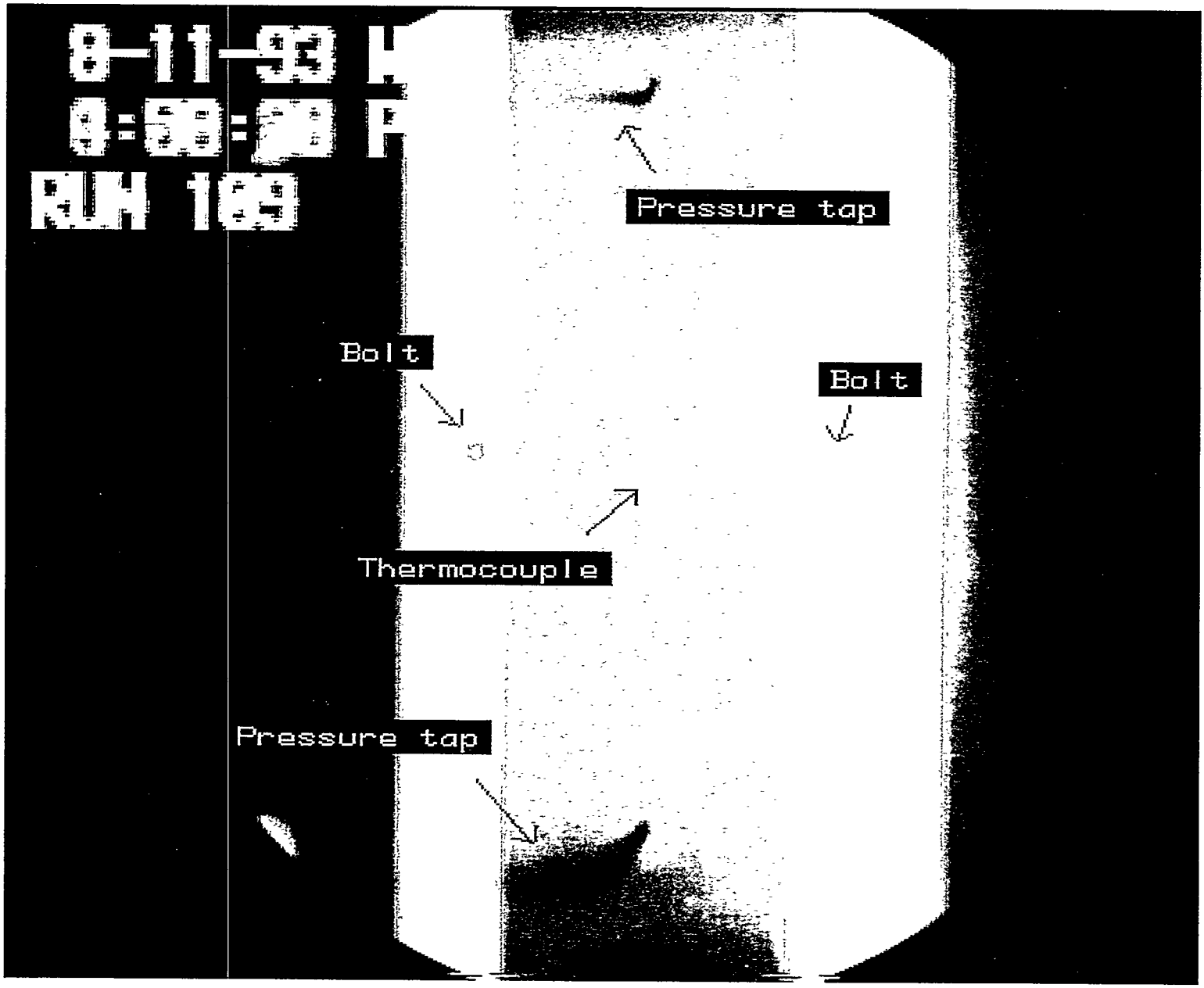

Figure 4 Time averaged radiograph of test region from which vapor fraction is determined.

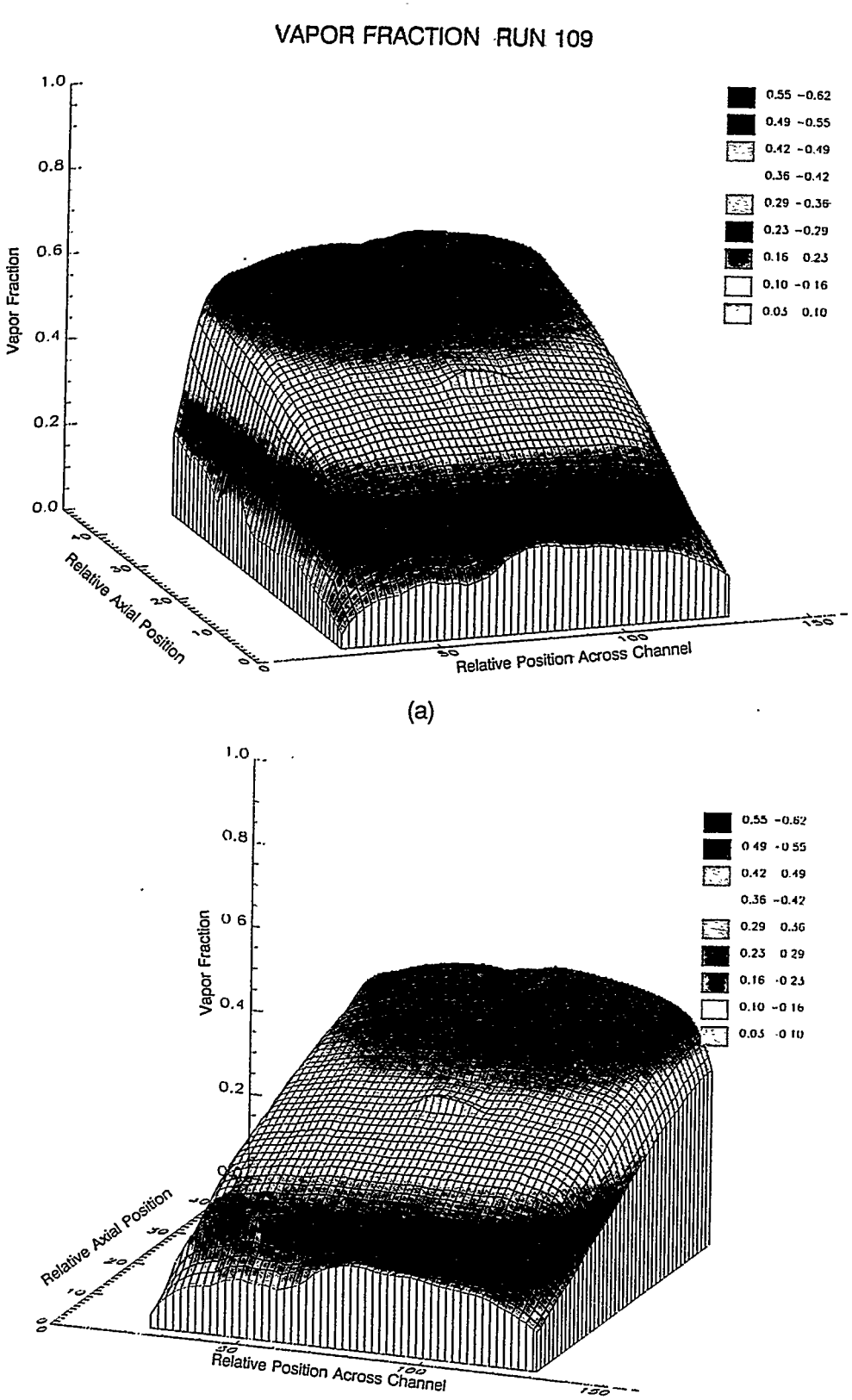

Figure 5 Typical 3-D representation of time-averaged vapor fraction results across and up an 8-inch region of the test section a) 45° view, b) 135° view.

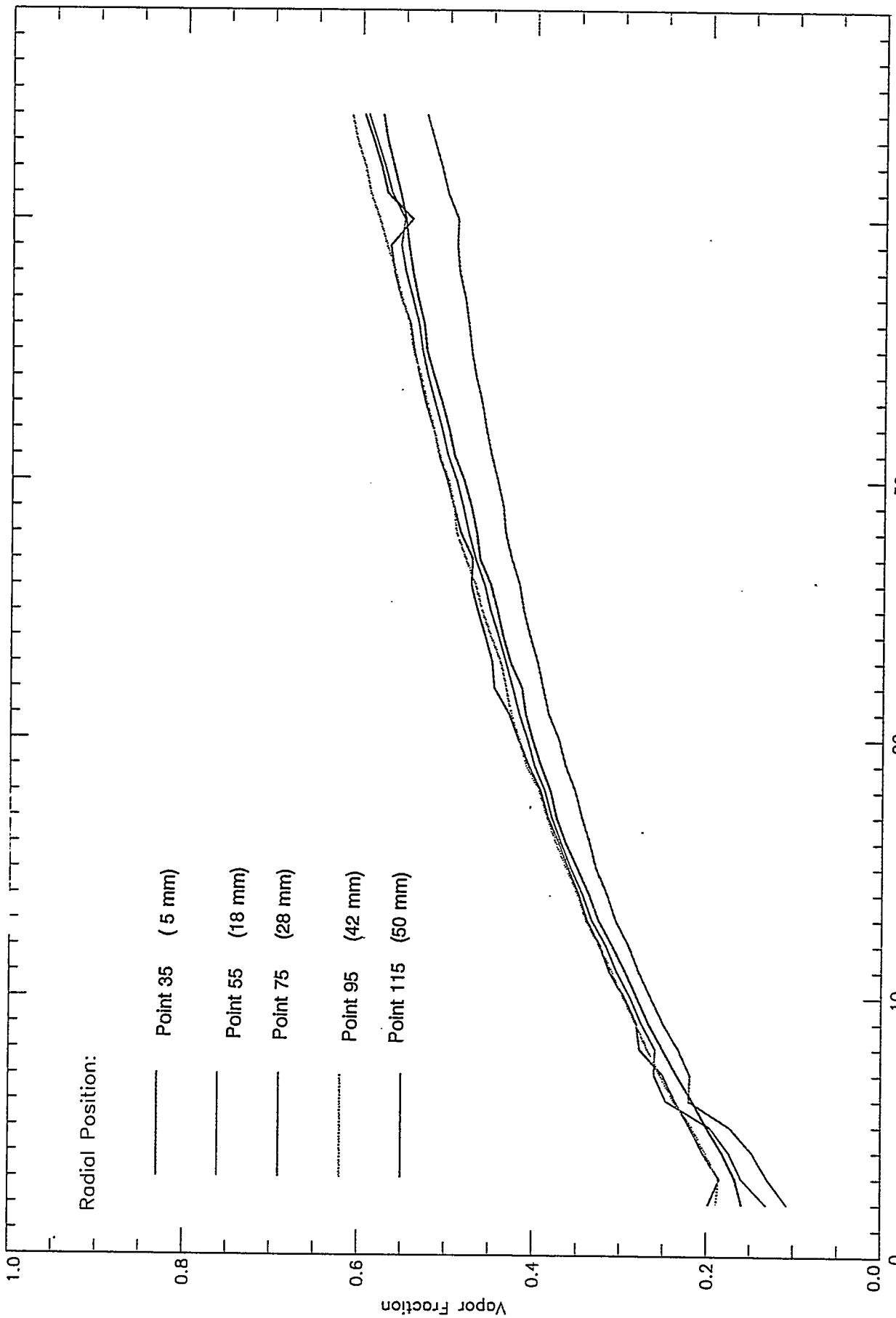

Figure 6 Plots of vapor fraction along test section for several relative radial position locations.

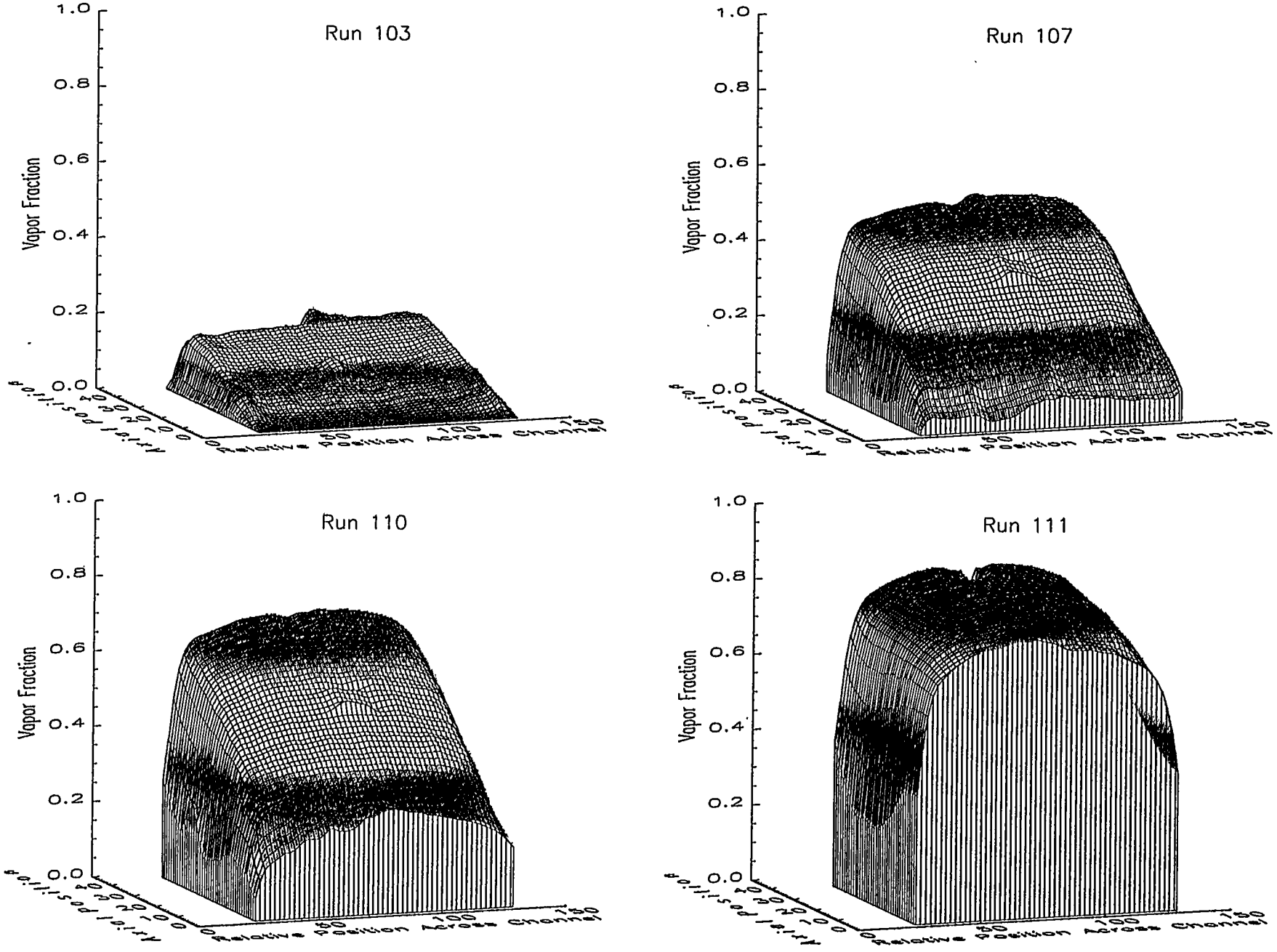

Figure 7 Vapor fraction measurements with increasing input heat (see Table 1).

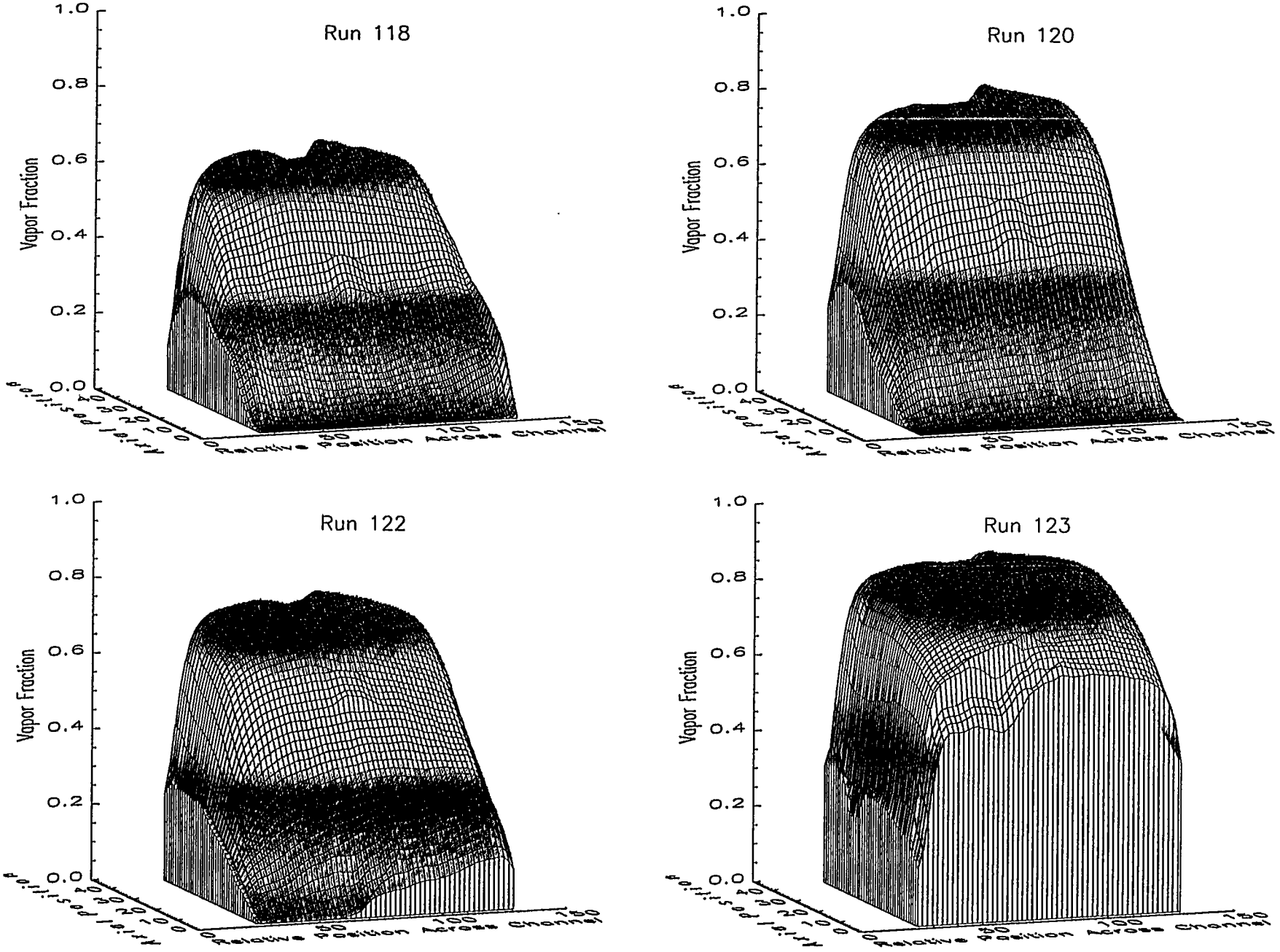

Figure 8 Vapor fraction measurements at other operating conditions (see Table 1).

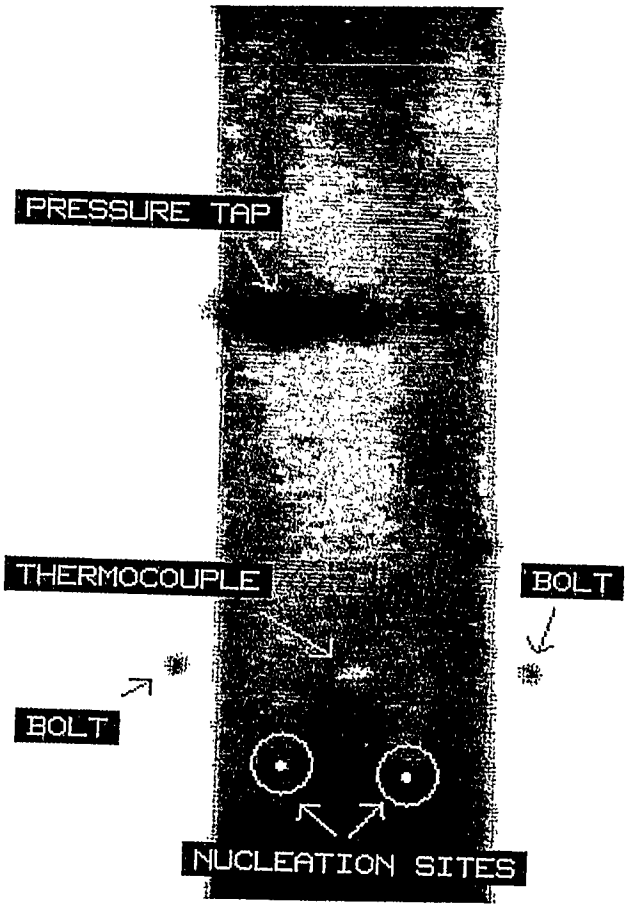

(a)

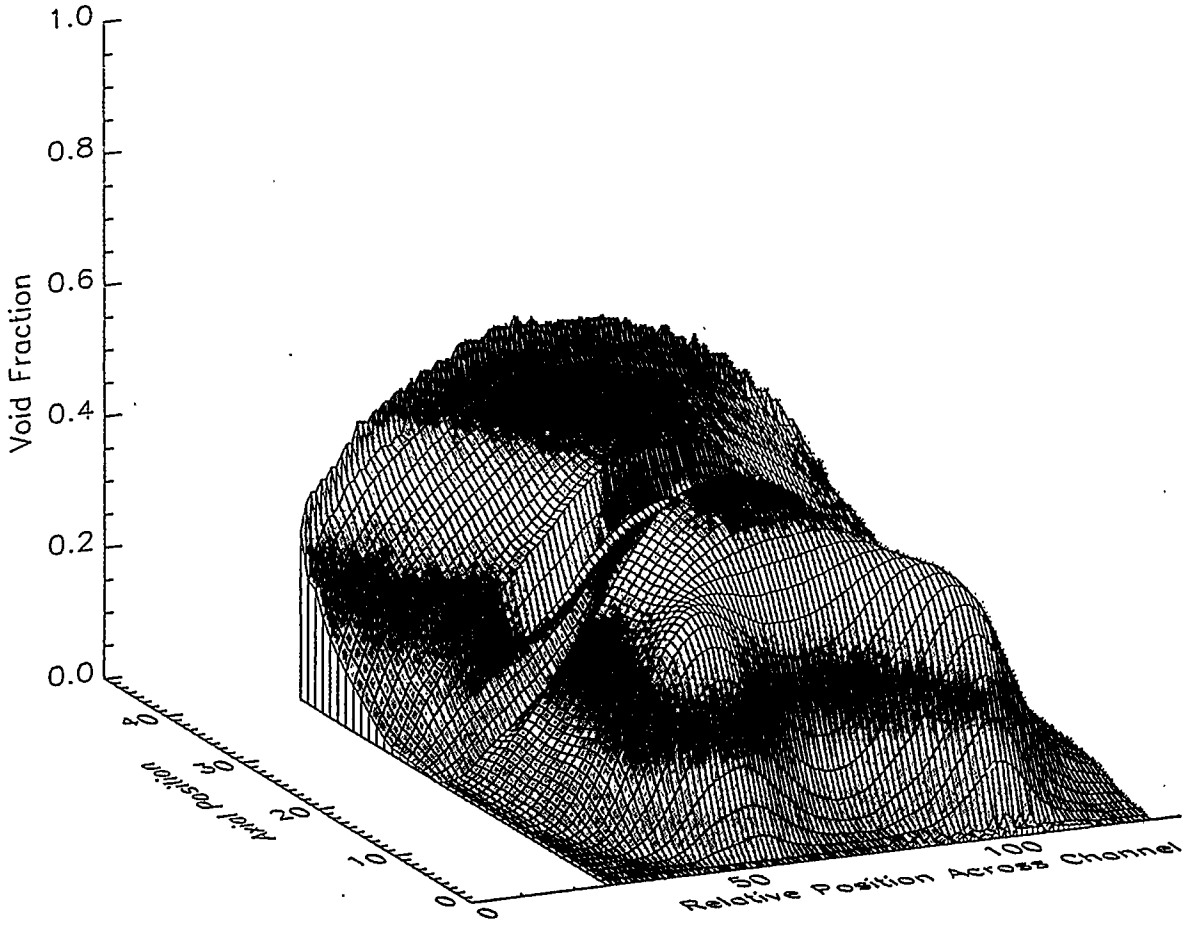

(b)

Figure 9 Unique results showing individual nucleation sites a) single frame radiograph of an 8-inch region of the test section, b) 3-D representation of time-averaged vapor fraction in the region of two nucleation sites. Depression at the center is an aberration due to pressure tap tubing on the outside of the test section.

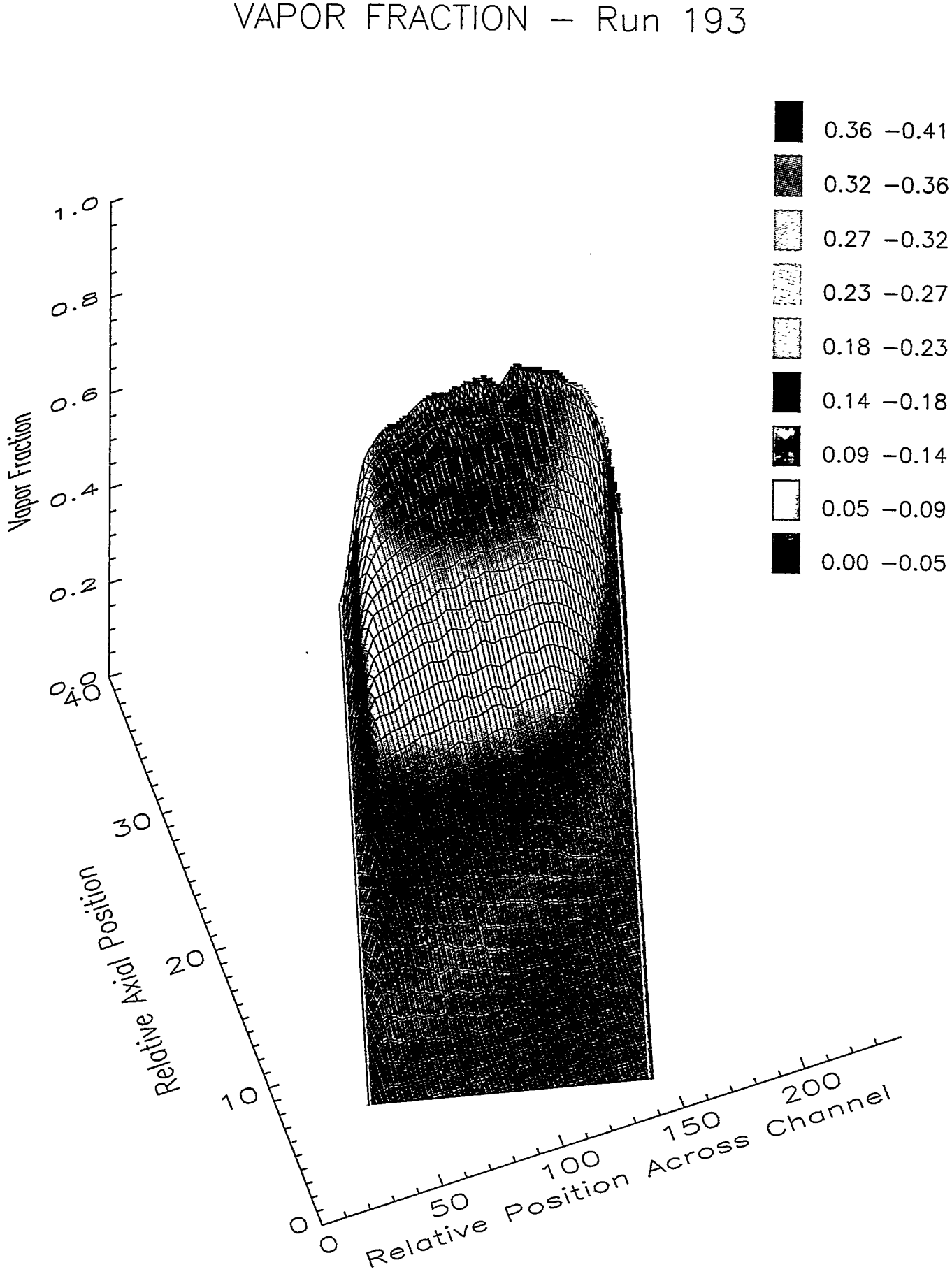

Figure 10 Typical time averaged vapor fraction with test section inclined 15°